# Dynamical Tunneling — Theory and Experiment

Srihari Keshavamurthy and Peter Schlagheck (eds)

January 29, 2010

# Contents

# Chapter 1

# Resonance-assisted tunneling in mixed regular-chaotic systems

## 1.1 Introduction

Since the early days of quantum mechanics, tunneling has been recognized as one of the hallmarks of the wave character of microscopic physics. The possibility of a quantum particle to penetrate an energetic barrier represents certainly one of the most spectacular implications of quantum theory and has lead to various applications in atomic and molecular physics as well as in mesoscopic science. Typical scenarios in which tunneling manifests are the escape of a quantum particle from a quasi-bound region, the transition between two or more symmetry-related, but classically disconnected wells (which we shall focus on in the following), as well as scattering or transport through potential barriers. The spectrum of scenarios becomes even richer when the concept of tunneling is generalized to any kind of classically forbidden transitions in phase space, i.e. to transitions that are not necessarily inhibited by static potential barriers but by some other constraints of the underlying classical dynamics (such as integrals of motion). Such "dynamical tunneling" processes arise frequently in molecular systems [1] and were realized with cold atoms propagating in periodically modulated optical lattices [2, 3].

Despite its genuinely quantal nature, tunneling is strongly influenced by the structure of the underlying classical phase space. (see Ref. [4] for a review). This is best illustrated within the textbook example of a one-dimensional symmetric double-well potential. In this simple case, the eigenvalue problem can be straightforwardly solved with the standard Wentzel-Kramers-Brillouin (WKB) ansatz [5]. The eigenstates of this system are, below the barrier height, obtained by the symmetric and antisymmetric linear combination of the local "quasi-modes" (i.e., of the wave functions that are semiclassically constructed on the quantized orbits within each well, without taking into account the classically forbidden coupling between the wells), and the splitting of their energies is given by an expression of the form

$$\Delta E = \frac{\hbar\omega}{\pi} \exp\left[-\frac{1}{\hbar}\int \sqrt{2m(V(x)-E)}dx\right] . \tag{1.1}$$

Here $E$ is the mean energy of the doublet, $V(x)$ represents the double well potential, $m$ is the

mass of the particle, $\omega$ denotes the oscillation frequency within each well, and the integral in the exponent is performed over the whole classically forbidden domain, i.e. between the inner turning points of the orbits in the two wells. Preparing the initial state as one of the quasi-modes (i.e., as the even or odd superposition of the symmetric and the antisymmetric eigenstate), the system will undergo Rabi oscillations between the wells with the frequency $\Delta E/\hbar$. The "tunneling rate" of this system is therefore given by the splitting (1.1) and decreases, keeping all classical parameters fixed, exponentially with $1/\hbar$, what gives rise to the statement that tunneling "vanishes" in the classical limit.

This approach can be generalized to multidimensional, even non separable systems, as long as their classical dynamics is still integrable [6]. It breaks down, however, as soon as a non-integrable perturbation is added to the system, e.g. if the one-dimensional double-well potential is exposed to a periodically time-dependent driving. In that case, the classical phase space of the system generally becomes mixed regular-chaotic. As visualized by the stroboscopic Poincaré section that is obtained through monitoring the phase space variables at fixed phases of the driving field, it typically displays two prominent regions of regular motion, corresponding to the weakly perturbed dynamics within the two wells, and a small (or, for stronger perturbations, large) layer of chaotic dynamics that separates the two regular islands from each other. Numerical calculations of model systems in the early nineties [7, 8] have shown that the tunnel splittings in such mixed systems generally become strongly enhanced compared to the integrable limit. Moreover, they do no longer follow a smooth exponential scaling with $1/\hbar$ as expressed by Eq. (1.1), but display huge, quasi-erratic fluctuations at variations of $\hbar$ or any other parameter of the system [7, 8].

These phenomena are traced back to the specific role that *chaotic* states play in such systems [9, 10, 11, 12]. In contrast to the integrable case, the tunnel doublets of the localized quasi-modes are, in a mixed regular-chaotic system, no longer isolated in the spectrum, but resonantly interact with states that are associated with the chaotic part of phase space. Due to their delocalized nature, such chaotic states typically exhibit a significant overlap with the boundary regions of both regular wells. They may therefore provide an efficient coupling mechanism between the quasi-modes – which becomes particularly effective whenever one of the chaotic levels is shifted exactly on resonance with the tunnel doublet. This coupling mechanism generally enhances the tunneling rate, but may also lead to a complete suppression thereof, arising at specific values of $\hbar$ or other parameters [13].

The validity of this "chaos-assisted" tunneling picture was essentially confirmed by a simple statistical ansatz in which the quantum dynamics within the chaotic part of the phase space was represented by a random matrix from the Gaussian orthogonal ensemble (GOE) [9, 10, 14]. In presence of small coupling coefficients between the regular states and the chaotic domain, this random matrix ansatz yields a truncated Cauchy distribution for the probability density to obtain a level splitting of the size $\Delta E$. Such a distribution is indeed encountered in the exact quantum splittings, which was demonstrated for the two-dimensional quartic oscillator [14] as well as, later on, for the driven pendulum Hamiltonian that describes the tunneling process of cold atoms in periodically modulated optical lattices [15, 16]. A quantitative prediction of the *average* tunneling rate, however, was not possible in the above-mentioned theoretical works. As we shall argue later on, this average tunneling rate is directly connected to the coupling matrix element between the regular and the chaotic states, and the strength of this matrix element was unknown and introduced in an ad-hoc way.

A first step towards his latter problem was undertaken by Podolskiy and Narimanov [17] who derived an explicit semiclassical expression for the mean tunneling rate in a mixed

system by assuming a perfectly clean, harmonic-oscillator like dynamics within the regular island and a structureless chaotic sea outside the outermost invariant torus of the island. This expression turned out to be successful for the reproduction of the level splittings between near-degenerate optical modes that are associated with a pair of symmetric regular islands in a non integrable micro-cavity [17] (see also Ref. [18]). The application to dynamical tunneling process in periodically modulated optical lattices [17], for which splittings between the left- and the right-moving stable eigenmodes were calculated in Ref. [15], seems convincing for low and moderate values of $1/\hbar$, but reveals deviations deeper in the semiclassical regime where plateau structures arise in the tunneling rates. Further, and more severe, deviations were encountered in the application of this approach to tunneling processes in other model systems [19].

Bäcker, Ketzmerick, Löck, and coworkers [20, 21] recently undertook the effort to derive in a more rigorous manner the regular-to-chaotic coupling rate governing chaos-assisted tunneling. Their approach is based on the construction of an integrable approximation for the nonintegrable system, which is designed such that it accurately describes the motion within the regular islands under consideration. The coupling rate to the chaotic domain is then determined through the computation of matrix elements of the system's Hamiltonian within the eigenbasis of this integrable approximation [20]. This results in a smooth exponential-like decay of the average tunneling rate with $1/\hbar$, which was indeed found to be in very good agreement with the exact tunneling rates for quantum maps and billiards [20, 21]. Those systems, however, were designed such as to yield a "clean" mixed regular-chaotic phase space, containing a regular island and a chaotic region which both do not exhibit appreciable substructures [20, 21].

In more generic systems, such as the quantum kicked rotor or the driven pendulum [15], however, even the "average" quantum tunneling rates do not exhibit a smooth monotonous behaviour with $1/\hbar$, but display peaks and plateau structures that cannot be accounted for by the above approaches. To understand the origin of such plateaus, it is instructive to step back to the conceptually simpler case of *nearly integrable* dynamics, where the perturbation from the integrable Hamiltonian is sufficiently small such that macroscopically large chaotic layers are not yet developed in the Poincaré surface of section. In such systems, the main effect of the perturbation consists in the manifestation of chain-like substructures in the phase space, which arise at *nonlinear resonances* between the eigenmodes of the unperturbed Hamiltonian, or, in periodically driven systems, between the external driving and the unperturbed oscillation within the well. In a similar way as for the quantum pendulum Hamiltonian, such resonances induce additional tunneling paths in the phase space, which lead to couplings between states that are located in the *same* well [22, 23].

The relevance of this effect for the near-integrable tunneling process between two symmetry-related wells was first pointed out by Bonci et al. [24] who argued that such resonances may lead to a strong enhancement of the tunneling rate, due to couplings between lowly and highly excited states within the well which are permitted by near-degeneracies in the spectrum. In Refs. [25, 26], a quantitative semiclassical theory of near-integrable tunneling was formulated on the basis of this principal mechanism. This theory allows one to reproduce the exact quantum splittings on the basis of purely classical quantities that can be extracted from the phase space, and takes into account high-order effects such as the coupling via a sequence of different resonance chains [25, 26]. More recent studies by Keshavamurthy on classically forbidden coupling processes in model Hamiltonians that mimic the dynamics of simple molecules confirm that the "resonance-assisted" tunneling scenario prevails not only in one-dimensional systems that are subject to a periodic driving (such as the "kicked Harper" model which was studied in Ref. [25, 26]), but also in autonomous systems with two

and even three degrees of freedom [27, 28].

...

## 1.2 Theory of resonance-assisted tunneling

### 1.2.1 Secular perturbation theory

For our study, we restrict ourselves to systems with one degree of freedom that evolve under a periodically time-dependent Hamiltonian $H(p,q,t) = H(p,q,t+\tau)$. We suppose that, for a suitable choice of parameters, the classical phase space of $H$ is mixed regular-chaotic and exhibits two symmetry-related regular islands that are embedded within the chaotic sea. This phase space structure is most conveniently visualized by a stroboscopic Poincaré section, where $p$ and $q$ are plotted at the times $t = n\tau (n \in \mathbb{Z})$. Such a Poincaré section typically reveals the presence of chain-like substructures within the regular islands, which arise due to nonlinear resonances between the external driving and the internal oscillation around the island's center. We shall assume now that the two islands exhibit a prominent $r$:$s$ resonance, i.e., a nonlinear resonance where $s$ internal oscillation periods match $r$ driving periods and $r$ sub-islands are visible in the stroboscopic section.

The classical motion in the vicinity of the $r$:$s$ resonance is approximately integrated by secular perturbation theory [29] (see also Ref. [26]). For this purpose, we formally introduce a time-independent Hamiltonian $H_0(p,q)$ that approximately reproduces the regular motion in the islands and preserves the discrete symmetry of $H$. The phase space generated by this integrable Hamiltonian consequently exhibits two symmetric wells that are separated by an energetic barrier and "embed" the two islands of $H$. In terms of the action-angle variables $(I,\theta)$ describing the dynamics within each of the wells, the total Hamiltonian can be written as

$$H(I,\theta,t) = H_0(I) + V(I,\theta,t) \tag{1.2}$$

where $V$ would represent a weak perturbation in the center of the island [30].

The nonlinear $r$:$s$ resonance occurs at the action variable $I_{r:s}$ that satisfies the condition

$$r\Omega_{r:s} = s\omega \tag{1.3}$$

with $\omega = 2\pi/\tau$ and

$$\Omega_{r:s} \equiv \left.\frac{dH_0}{dI}\right|_{I=I_{r:s}} . \tag{1.4}$$

We now perform a canonical transformation to the frame that corotates with this resonance. This is done by leaving $I$ invariant and modifying $\theta$ according to

$$\theta \mapsto \vartheta = \theta - \Omega_{r:s} t \, . \tag{1.5}$$

This time-dependent shift is accompanied by the transformation $H \mapsto \mathcal{H} = H - \Omega_{r:s} I$ in order to ensure that the new corotating angle variable $\vartheta$ is conjugate to $I$. The motion of $I$ and $\vartheta$ is therefore described by the new Hamiltonian

$$\mathcal{H}(I,\vartheta,t) = \mathcal{H}_0(I) + \mathcal{V}(I,\vartheta,t) \tag{1.6}$$

with

$$\mathcal{H}_0(I) = H_0(I) - \Omega_{r:s} I \,, \tag{1.7}$$
$$\mathcal{V}(I,\vartheta,t) = V(I,\vartheta+\Omega_{r:s}t,t) \,. \tag{1.8}$$

The expansion of $\mathcal{H}_0$ in powers of $I - I_{r:s}$ yields

$$\mathcal{H}_0(I) \simeq \mathcal{H}_0^{(0)} + \frac{(I-I_{r:s})^2}{2m_{r:s}} + \mathcal{O}\left[(I-I_{r:s})^3\right] \tag{1.9}$$

with a constant $\mathcal{H}_0^{(0)} \equiv H_0(I_{r:s}) - \Omega_{r:s} I_{r:s}$ and a quadratic term that is characterized by the effective "mass" parameter $m_{r:s}$. Hence, $d\mathcal{H}_0/dI$ is comparatively small for $I \simeq I_{r:s}$, which implies that the corotating angle $\vartheta$ varies slowly in time near the resonance. This justifies the application of adiabatic perturbation theory [29], which effectively amounts, in first order, to replacing $\mathcal{V}(I,\vartheta,t)$ by its time average over $r$ periods of the driving (using the fact that $\mathcal{V}$ is periodic in $t$ with the period $r\tau$) [31]. We therefore obtain, after this transformation, the time-independent Hamiltonian

$$\mathcal{H}(I,\vartheta) = \mathcal{H}_0(I) + \mathcal{V}(I,\vartheta) \tag{1.10}$$

with

$$\mathcal{V}(I,\vartheta) \equiv \frac{1}{r\tau}\int_0^{r\tau} \mathcal{V}(I,\vartheta,t)dt \,. \tag{1.11}$$

By making a Fourier series expansion for $V(I,\theta,t)$ in both $\theta$ and $t$, i.e.

$$V(I,\theta,t) = \sum_{l,m=-\infty}^{\infty} V_{l,m}(I) e^{il\theta} e^{im\omega t} \tag{1.12}$$

with $V_{l,m}(I) = [V_{-l,-m}(I)]^*$, one can straightforwardly derive

$$\mathcal{V}(I,\vartheta) = V_{0,0}(I) + \sum_{k=0}^{\infty} 2V_k(I)\cos(kr\vartheta + \phi_k) \tag{1.13}$$

defining

$$V_k(I)e^{i\phi_k} \equiv V_{rk,-sk}(I) \,, \tag{1.14}$$

i.e., the resulting time-independent perturbation term is $(2\pi/r)$-periodic in $\vartheta$.

In a first step, we neglect the action dependence of the Fourier coefficients of $\mathcal{V}(i,\vartheta)$ and replace $V_k(I)$ by $V_k \equiv V_k(I = I_{r:s})$ in Eq. (1.13). Neglecting furthermore the term $V_{0,0}(I)$, we obtain the effective integrable Hamiltonian

$$H_{\text{eff}}(I,\vartheta) = H_0(I) - \Omega_{r:s} I + \sum_{k=1}^{\infty} 2V_k \cos(kr\vartheta + \phi_k) \tag{1.15}$$

for the description of the classical dynamics in the vicinity of the resonance.

### 1.2.2 The pendulum approximation

The quantum implications due to the presence of this nonlinear resonance can be straightforwardly inferred from the direct semiclassical quantization of $H_{\rm eff}$, given by

$$\hat{H}_{\rm eff} = H_0(\hat{I}) - \Omega_{r:s}\hat{I} + \sum_{k=1}^{\infty} 2V_k \cos(kr\hat{\vartheta} + \phi_k)\,. \tag{1.16}$$

Here we introduce the action operator $\hat{I} \equiv -i\hbar\partial/\partial\vartheta$ and assume anti-periodic boundary conditions in $\vartheta$ in order to properly account for the Maslov index in the original phase space [22]. In accordance with our assumption that the effect of the resonance is rather weak, we can now apply quantum perturbation theory to the Hamiltonian (1.16), treating the $\hat{I}$-dependent "kinetic" terms as unperturbed part, with the unperturbed eigenstates $\langle\vartheta|n\rangle = \exp[i(n+0.5)\vartheta]$, and the $\hat{\vartheta}$-dependent series as perturbation. The unperturbed eigenstates are then given by the (anti-periodic) eigenfunctions $\langle\vartheta|n\rangle = \exp[i(n+0.5)\vartheta]$ ($n \geq 0$) of the action operator $\hat{I}$ with the eigenvalues

$$I_n = \hbar(n + 1/2)\,. \tag{1.17}$$

As is straightforwardly evaluated, the presence of the perturbation induces couplings between the states $|n\rangle$ and $|n+kr\rangle$ with the matrix elements

$$\langle n+kr|\hat{H}_{\rm eff}|n\rangle = V_k e^{i\phi_k} \tag{1.18}$$

for positive $k$. As a consequence, the "true" eigenstates $|\psi_n\rangle$ of $\hat{H}_{\rm eff}$ contain admixtures from unperturbed modes $|n'\rangle$ that satisfy the selection rule $|n'-n| = kr$ with integer $k$. They are approximated by the expression

$$\begin{aligned} |\psi_n\rangle \;=\; & |n\rangle + \sum_{k\neq 0} \frac{\langle n+kr|\hat{H}_{\rm eff}|n\rangle}{E_n - E_{n+kr} + ks\hbar\omega}|n+kr\rangle + \\ & + \sum_{k,k'\neq 0} \frac{\langle n+kr|\hat{H}_{\rm eff}|n+k'r\rangle}{E_n - E_{n+kr} + ks\hbar\omega}\frac{\langle n+k'r|\hat{H}_{\rm eff}|n\rangle}{E_n - E_{n+k'r} + k's\hbar\omega}|n+kr\rangle + \ldots \end{aligned} \tag{1.19}$$

where $E_n \equiv H_0(I_n)$ denote the unperturbed eigenenergies of $H_0$ and the resonance condition (1.3) is used.

Within the quadratic approximation of $H_0(I)$ around $I_{r:s}$, we obtain from Eqs. (1.7) and (1.8)

$$E_n \simeq H_0(I_{r:s}) - \Omega_{r:s}(I_n - I_{r:s}) + \frac{1}{2m_{r:s}}(I_n - I_{r:s})^2\,. \tag{1.20}$$

This results in the energy differences

$$E_n - E_{n+kr} + ks\hbar\omega \simeq \frac{1}{2m_{r:s}}(I_n - I_{n+kr})(I_n + I_{n+kr} - 2I_{r:s})\,. \tag{1.21}$$

From this expression, we see that the admixture between $|n\rangle$ and $|n'\rangle$ becomes particularly strong if the $r$:$s$ resonance is symmetrically located between the two tori that are associated

with the actions $I_n$ and $I_{n'}$ — i.e., if $I_n + I_{n'} \simeq 2I_{r:s}$. The presence of a significant nonlinear resonance within a region of regular motion provides therefore an efficient mechanism to couple the local "ground state" — i.e, the state that is semiclassically localized in the center of that region (with action variable $I_0 < I_{r:s}$) — to a highly excited state (with action variable $I_{kr} > I_{r:s}$).

It is instructive to realize that the Fourier coefficients $V_k$ of the perturbation operator decrease rather rapidly with increasing $k$. Indeed, one can derive under quite general circumstances the asymptotic scaling law

$$V_k \sim (kr)^\gamma V_0 \exp[-kr\Omega_{r:s} t_{\rm im}(I_{r:s})] \tag{1.22}$$

for large $k$, which is based on the presence of singularities of the complexified tori of the integrable approximation $H_0(I)$ [26]. Here $t_{\rm im}(I)$ denotes the imaginary time that elapses from the (real) torus with action $I$ to the nearest singularity in complex phase space, $\gamma$ corresponds to the degree of the singularity, and $V_0$ contains information about the corresponding residue near the singularity as well as the strength of the perturbation. The expression (1.22) is of little practical relevance as far as the concrete determination of the coefficients $V_k$ is concerned. It permits, however, to estimate the relative importance of different perturbative pathways connecting the states $|n\rangle$ and $|n+kr\rangle$ in Eq. (1.19). Comparing e.g. the amplitude $\mathcal{A}_2$ associated with a single step from $|n\rangle$ to $|n+2r\rangle$ via $V_2$ and the amplitude $\mathcal{A}_1$ associated with two steps from $|n\rangle$ to $|n+2r\rangle$ via $V_1$, we obtain from Eqs. (1.21) and (1.22) the ratio

$$\mathcal{A}_2/\mathcal{A}_1 \simeq \frac{2^\gamma r^{2-\gamma}\hbar^2}{m_{r:s}V_0} e^{i(\phi_2-2\phi_1)} \tag{1.23}$$

under the assumption that the resonance is symmetrically located in between the corresponding two tori. Since $V_0$ can be assumed to be finite in mixed regular-chaotic systems, we infer that the second-order process via the stronger coefficient $V_1$ will more dominantly contribute to the coupling between $|n\rangle$ and $|n+2r\rangle$ in the semiclassical limit $\hbar \to 0$.

A similar result is obtained from a comparison of the one-step process via $V_k$ with the $k$-step process via $V_1$, where we again find that the latter more dominantly contributes to the coupling between $|n\rangle$ and $|n+kr\rangle$ in the limit $\hbar \to 0$. We therefore conclude that in mixed regular-chaotic systems the semiclassical tunneling process is adequately described by the lowest nonvanishing term of the sum over the $V_k$ contributions, which in general is given by $V_1 \cos(r\vartheta + \phi_1)$ [32]. Neglecting all higher Fourier components $V_k$ with $k > 1$ and making the quadratic approximation of $H_0$ around $I = I_{r:s}$, we finally obtain an effective pendulum-like Hamiltonian

$$H_{\rm eff}(I,\vartheta) \simeq \frac{(I-I_{r:s})^2}{2m_{r:s}} + 2V_{r:s}\cos(r\vartheta + \phi_1) \tag{1.24}$$

with $V_{r:s} \equiv V_1$ [33].

This simple form of the effective Hamiltonian allows us to determine the parameters $I_{r:s}$, $m_{r:s}$ and $V_{r:s}$ from the Poincaré map of the classical dynamics, without explicitly using the transformation to the action-angle variables of $H_0$. To this end, we numerically calculate the monodromy matrix $M_{r:s} \equiv \partial(p_f, q_f)/\partial(p_i, q_i)$ of a stable periodic point of the resonance (which involves $r$ iterations of the stroboscopic map) as well as the phase space areas $S^+_{r:s}$ and $S^-_{r:s}$ that are enclosed by the outer and inner separatrices of the resonance, respectively (see also Fig. 1.1). Using the fact that the trace of $M_{r:s}$ as well as the phase space areas $S^\pm_{r:s}$

remain invariant under the canonical transformation to $(I, \vartheta)$, we infer

$$I_{r:s} = \frac{1}{4\pi}(S^+_{r:s} + S^-_{r:s}), \tag{1.25}$$

$$\sqrt{2m_{r:s}V_{r:s}} = \frac{1}{16}(S^+_{r:s} - S^-_{r:s}), \tag{1.26}$$

$$\sqrt{\frac{2V_{r:s}}{m_{r:s}}} = \frac{1}{r^2\tau}\arccos(\mathrm{tr}\, M_{r:s}/2) \tag{1.27}$$

from the integration of the dynamics generated by $H_{\mathrm{eff}}$ [34].

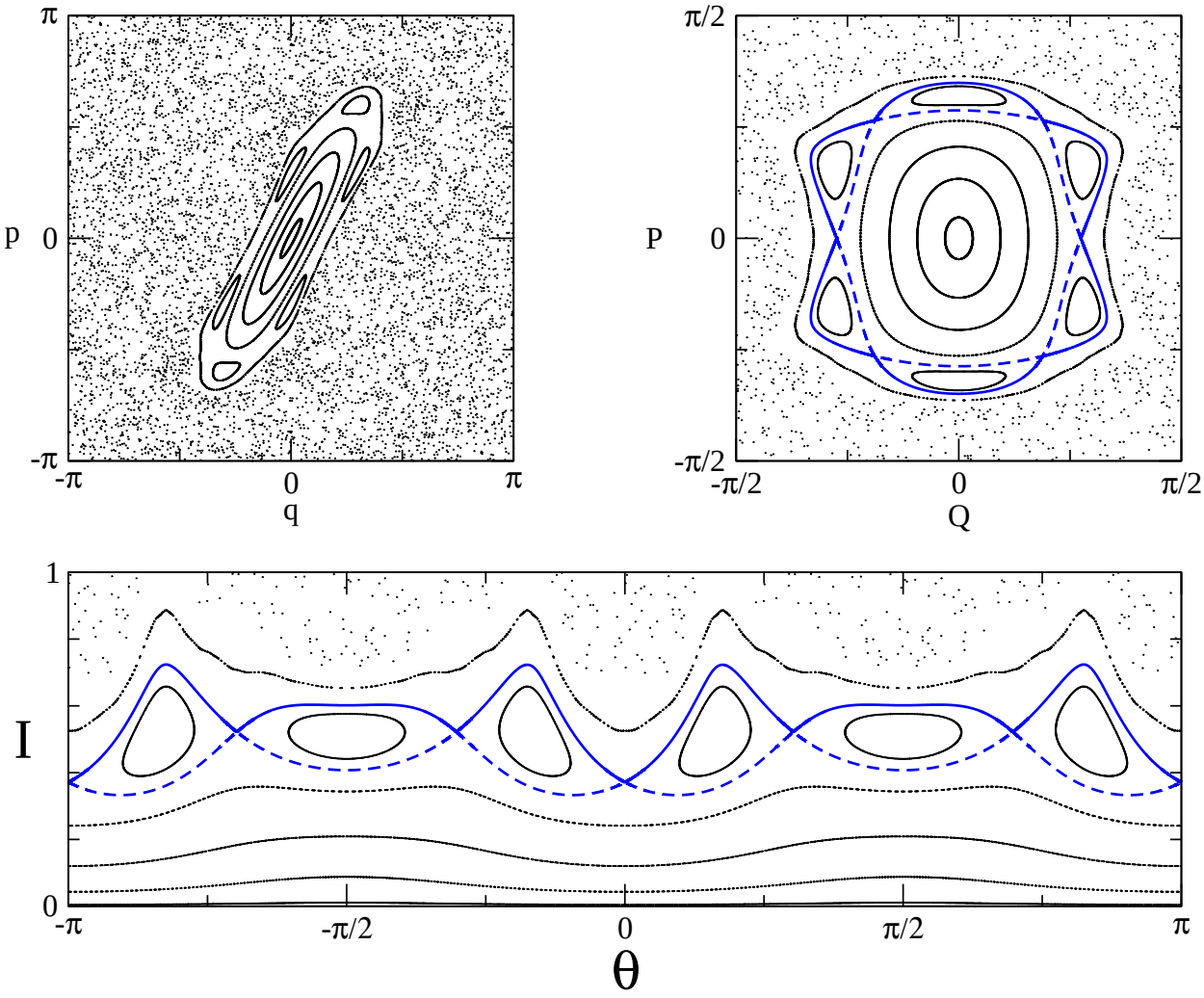


Figure 1.1: Classical phase space of the kicked rotor Hamiltonian at $K = 3.5$ showing a regular island with an embedded 6:2 resonance. The phase space is plotted in the original $(p, q)$ coordinates (upper left panel), in approximate normal-form corrdinates $(P, Q)$ (upper right panel), and in approximate action-angle variables $(I, \vartheta)$ (lower panel). The blue solid and dashed lines represent the "outer" and "inner" separatrix of the resonance, respectively.

### 1.2.3 Action dependence of the coupling coefficients

Up to now, and in our previous publications [25, 26, 33, 35, 36], we completely neglected the action dependence of the coupling coefficients $V_k(I)$. This approximation should be justified in the semiclassical limit of extremely small $\hbar$, where resonance-assisted tunneling generally involves multiple coupling processes [26] and transitions across individual resonance chains are therefore expected to take place in their immediate vicinity in action space. For finite $\hbar$, however, the replacement $V_k(I) \mapsto V_k(I_{r:s})$, permitting the direct quantization in action-angle space, is, in general, not sufficient to obtain an accurate reproduction of the quantum tunneling rates. We show now how this can be improved.

To this end, we make the general assumption that the classical Hamiltonian $H(p,q,t)$ of our system is analytic in $p$ and $q$ in the vicinity of the regular islands under consideration. It is then possible to define an analytical canonical transformation from $(p,q)$ to Birkhoff-Gustavson normal-form coordinates $(P,Q)$ [37, 38] that satisfy

$$P = -\sqrt{2I}\sin\theta\,, \tag{1.28}$$

$$Q = \sqrt{2I}\cos\theta \tag{1.29}$$

and that can be represented in power series in $p$ and $q$. The "unperturbed" integrable Hamiltonian $H_0$ therefore depends only on $I = (P^2+Q^2)/2$.

Writing

$$e^{\pm il\theta} = \left(\frac{Q \mp iP}{\sqrt{2I}}\right)^l \tag{1.30}$$

for positive $l$, we obtain, from Eq. (1.12), the series

$$V(I,\theta,t) = \sum_{m=-\infty}^{\infty}\left\{V_{0,m}(I) + \sum_{l=1}^{\infty}\frac{1}{\sqrt{2I}^l}\left[V_{l,m}(I)(Q-iP)^l + V_{-l,m}(I)(Q+iP)^l\right]\right\}e^{im\omega t} \tag{1.31}$$

for the perturbation. Using the fact that $V(I,\theta,t)$ is analytic in $P$ and $Q$, we infer that $V_{l,m}(I)$ must scale at least proportional to $I^{l/2}$ with $I$. By virtue of (1.14), this implies the scaling $V_k(I) \propto I^{rk/2}$ for the Fourier coefficients of the time-independent perturbation term that is associated with the $r{:}s$ resonance. Making the ansatz $V_k(I) \equiv I^{rk/2}\tilde{v}_k$ (and neglecting the residual action dependence of $\tilde{v}_k$), we rewrite Eq. (1.13) as [39]

$$\mathcal{V}(I,\vartheta) = V_{0,0}(I) + \sum_{k=0}^{\infty}\frac{\tilde{v}_k}{2^{kr/2}}\left[(Q-iP)^{kr}e^{i\phi_k} + (Q+iP)^{kr}e^{-i\phi_k}\right]. \tag{1.32}$$

The quantization of the resulting classical Hamiltonian can now be carried out in terms of the "harmonic oscillator" variables $P$ and $Q$ and amounts to introducing the standard ladder operators $\hat{a}$ and $\hat{a}^\dagger$ according to

$$\hat{a} = \frac{1}{\sqrt{2\hbar}}(\hat{Q} + i\hat{P})\,, \tag{1.33}$$

$$\hat{a}^\dagger = \frac{1}{\sqrt{2\hbar}}(\hat{Q} - i\hat{P})\,. \tag{1.34}$$

This yields the quantum Hamiltonian

$$\hat{H}_{\rm eff} = H_0(\hat{I}) - \Omega_{r:s}\hat{I} + \sum_{k=1}^{\infty} \tilde{v}_k \hbar^{kr/2} \left[\hat{a}^{kr} e^{-i\phi_k} + (\hat{a}^\dagger)^{kr} e^{i\phi_k}\right] \tag{1.35}$$

with $\hat{I} \equiv \hbar(\hat{a}^\dagger\hat{a}+1/2)$. As for Eq. (1.16), perturbative couplings are introduced only between unperturbed eigenstates $|n\rangle$ and $|n'\rangle$ that exhibit the selection rule $|n'-n| = kr$ with integer $k$. The associated coupling matrix elements are, however, different from Eq. (1.18) and read

$$\begin{aligned} \langle n+kr|\hat{H}_{\rm eff}|n\rangle &= \tilde{v}_k \sqrt{\hbar}^{kr} e^{i\phi_k} \sqrt{\frac{(n+kr)!}{n!}} \\ &= V_k(I_{r:s}) e^{i\phi_k} \left(\frac{\hbar}{I_{r:s}}\right)^{kr/2} \sqrt{\frac{(n+kr)!}{n!}} \end{aligned} \tag{1.36}$$

for positive $k$. This difference becomes particularly pronounced if the $r$:$s$ resonance is, in phase space, rather asymmetrically located in between the invariant tori that correspond to the states $|n\rangle$ and $|n+kr\rangle$ — i.e., if $I_{r:s}$ is rather close to $I_n$ or to $I_{n+kr}$. In that case, Eq. (1.18) may, respectively, strongly over- or underestimate the coupling strength between these states.

### 1.2.4 Chaos-assisted tunneling

We now discuss the implication of such nonlinear resonances on the tunneling process between the two symmetry-related regular islands under consideration. In the quantum system, these islands support (for not too large values of $\hbar$) locally quantized eigenstates or "quasimodes" with different node numbers $n$, which, due to the symmetry, have the same eigenvalues in both islands. In our case of a periodically driven system, these eigenvalues can be the eigenphases $\varphi_n$ of the unitary time evolution operator $U$ over one period $\tau$ of the driving, or, alternatively, the quasienergies $E_n$ that arise from the diagonalization of the corresponding Floquet operator. We generally have the relation $\varphi_n = -E_n\tau/\hbar \pmod{2\pi}$.

The presence of a small tunneling-induced coupling between the islands lifts the degeneracy of the eigenvalues and yields the symmetric and antisymmetric linear combination of the quasimodes in the two islands as "true" eigenstates of the system. A nonvanishing splitting $\Delta\varphi_n \equiv |\varphi_n^+ - \varphi_n^-|$ consequently arises between the eigenphases $\varphi_n^\pm$ of the symmetric and the antisymmetric state, which is related to the splitting $\Delta E_n \equiv |E_n^+ - E_n^-|$ of the quasienergies $E_n^\pm$ through $\Delta\varphi_n = \tau\Delta E_n/\hbar$. Within the integrable approximation of our driven system with one degree of freedom, these energy splittings can be semiclassically calculated from the integrable Hamiltonian $H_0$ via an analytic continuation of the invariant tori to the complex domain [6]. This generally yields the splittings

$$\Delta E_n^{(0)} = \frac{\hbar\Omega_n}{\pi} \exp(-\sigma_n/\hbar) \tag{1.37}$$

where $\Omega_n$ is the classical oscillation frequency associated with the $n$th quantized torus and $\sigma_n$ denotes the imaginary part of the action integral along the complex path that joins the two symmetry-related tori.

The main effect of nonlinear resonances in the nonintegrable system is, as was discussed in the previous subsections, to induce perturbative couplings between quasimodes of different excitation within the regular islands. This can lead to a substantial enhancement of the splittings $\Delta E_n$ as compared to Eq. (1.37) already for nearly integrable systems in which chaos is not yet visibly manifested in phase space [25, 26]. As can be straightforwardly derived within quantum perturbation theory, the modified splitting of the local "ground state" in the island (i.e., the state with vanishing node number $n = 0$) is in the presence of a prominent $r$:$s$ resonance given by

$$\Delta\varphi_0 = \Delta\varphi_0^{(0)} + \sum_k |\mathcal{A}_{kr}^{(r:s)}|^2 \Delta\varphi_{kr}^{(0)} \tag{1.38}$$

where $\mathcal{A}_{kr}^{(r:s)} \equiv \langle kr|\psi_0\rangle$ denotes the admixture of the $(kr)$th excited unperturbed component $|kr\rangle$ to the perturbed ground state $|\psi_0\rangle$ according to Eq. (1.19) [possibly using Eq. (1.36) instead of (1.18)]. The rapid decrease of the amplitudes $\mathcal{A}_{kr}^{(r:s)}$ with $k$ is compensated by an exponential increase of the unperturbed splittings $\Delta\varphi_{kr}^{(0)}$, arising from the fact that the tunnel action $\sigma_n$ in Eq. (1.37) generally decreases with increasing $n$. The maximal contribution to the modified ground state splitting is generally provided by the state $|kr\rangle$ for which $I_{kr} + I_0 \simeq 2I_{r:s}$ — i.e., which in phase space is most closely located to the torus that lies symmetrically on the opposite side of the resonance chain. This contribution is particularly enhanced by a small energy denominator [see Eq. (1.21] and typically dominates the sum in Eq. (1.38).

In the mixed regular-chaotic case, invariant tori exist only up to a maximum action variable $I_c$ corresponding to the outermost boundary of the regular island in phase space. Beyond this outermost invariant torus, multiple overlapping resonances provide various couplings and pathways such that unperturbed states in this regime can be assumed to be strongly connected to each other. Under such circumstances, the classically forbidden coupling between the two symmetric islands does not require any barrier tunneling process of the type (1.37). It can be achieved by any coupling process that connects the ground state, or any other "regular" state inside the island, to a state that is defined within the chaotic domain [9, 10].

A straightforward guess consists in stating that this coupling process is induced by the presence of one or several $r$:$s$ resonances within the island. This means that the ground state of the island is connected, through perturbative chains of the form (1.19), to highly excited quasimodes of the integrable approximation $H_0$ which are defined on invariant tori that become destroyed in the mixed regular-chaotic system. These latter quasimodes are, in the quantum system, therefore strongly coupled to each other and to their symmetric counterparts and thereby provide the breaking of the degeneracy between the symmetric and antisymmetric (quasi-)energies of the ground state doublet.

The structure of the effective Hamiltonian that describes this coupling process in the presence of a single nonlinear $r$:$s$ resonance is depicted in Fig. 1.2. Keeping in mind the discussion in Section 1.2.2 and in Ref. [26], we assume here that the couplings induced by the $r$:$s$ resonance are dominantly described by the lowest nonvanishing Fourier component $V_1$ of the perturbation, i.e. by the matrix elements $V_{r:s}^{(n+r)} \equiv \langle n+r|\hat{H}_{\rm eff}|n\rangle$, and set the phase $\phi_1$ to zero without loss of generality. Separating the Hilbert space into an "even" and "odd" subspace with respect to the discrete symmetry of $H$ and eliminating intermediate states

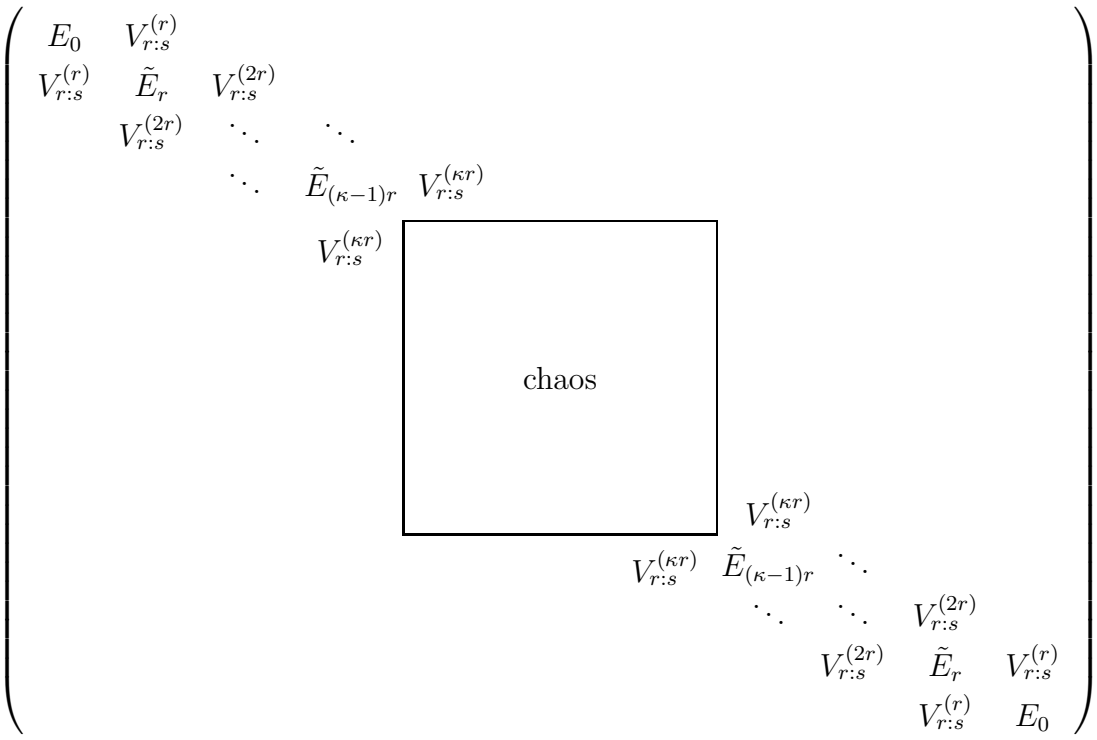


Figure 1.2: Sketch of the effective Hamiltonian matrix that describes tunneling between the symmetric quasi-modes in the two separate regular islands. The regular parts (upper left and lower right band) includes only components that are coupled to the island's ground state by the $r$:$s$ resonance. The chaotic part (central square) consists of a full sub-block with equally strong couplings between all basis states with actions beyond the outermost invariant torus of the islands. $\tilde{E}_{kr} \equiv E_{kr} - \Omega_{r:s} I_{kr}$ are the eigenenergies of the unperturbed Hamiltonian $\mathcal{H}_0$ in the co-rotating frame.

within the regular island leads to an effective Hamiltonian matrix of the form

$$H_{\text{eff}}^{\pm} = \begin{pmatrix} E_0 & V_{\text{eff}} & 0 & \cdots & 0 \\ V_{\text{eff}} & H_{11}^{\pm} & \cdots & \cdots & H_{1N}^{\pm} \\ 0 & \vdots & & & \vdots \\ \vdots & \vdots & & & \vdots \\ 0 & H_{N1}^{\pm} & \cdots & \cdots & H_{NN}^{\pm} \end{pmatrix} . \tag{1.39}$$

for each symmetry class. The effective coupling matrix element between the ground state and the chaos block ($H_{ij}^{\pm}$) is given by

$$V_{\text{eff}} = V_{r:s}^{(\kappa r)} \prod_{k=1}^{\kappa-1} \frac{V_{r:s}^{(kr)}}{E_0 - E_{kr} + ks\hbar\omega} \tag{1.40}$$

where $E_n$ are the unperturbed energies (1.20) of $H_{\text{eff}}$. Here $|\kappa r\rangle$ represents the lowest unperturbed state that is connected by the $r$:$s$ resonance to the ground state and located outside the outermost invariant torus of the island (i.e., $I_{(\kappa-1)r} < I_c < I_{\kappa r}$).

In the simplest possible approximation, which follows the lines of Refs. [10, 14], we neglect the effect of partial barriers in the chaotic part of the phase space [9] and assume that the chaos block ($H_{ij}^{\pm}$) is adequately modeled by a random hermitian matrix from the Gaussian orthogonal ensemble (GOE). After a pre-diagonalization of ($H_{ij}^{\pm}$), yielding the eigenstates $\phi_j^{\pm}$ and eigenenergies $\mathcal{E}_j^{\pm}$, we can perturbatively express the shifts of the symmetric and antisymmetric ground state energies by

$$E_0^{\pm} = E_0 + V_{\text{eff}}^2 \sum_{j=1}^{N} \frac{|\langle kr|\phi_j^{\pm}\rangle|^2}{E_0 - \mathcal{E}_j^{\pm}} \,. \tag{1.41}$$

Performing the random matrix average for the eigenvectors, we obtain

$$|\langle kr|\phi_j^{\pm}\rangle|^2 \simeq 1/N \tag{1.42}$$

for all $j = 1 \ldots N$, which simply expresses the fact that none of the basis states is distinguished within the chaotic block ($H_{ij}$).

As was shown in Ref. [14], the random matrix average over the eigenvalues $\mathcal{E}_j^{\pm}$ gives rise to a Cauchy distribution for the shifts of the ground state energies, and consequently also for the splittings

$$\Delta E_0 = |E_0^+ - E_0^-| \tag{1.43}$$

between the symmetric and the antisymmetric ground state energy. For the latter, we specifically obtain the probability distribution

$$P(\Delta E_0) = \frac{2}{\pi} \frac{\overline{\Delta E_0}}{(\Delta E_0)^2 + (\overline{\Delta E_0})^2} \tag{1.44}$$

with

$$\overline{\Delta E_0} = \frac{2\pi V_{\text{eff}}^2}{N \Delta_c} \tag{1.45}$$

where $\Delta_c$ denotes the mean level spacing in the chaos at energy $E_0$. This distribution is, strictly speaking, valid only for $\Delta E_0 \ll V_{\text{eff}}$ and exhibits a cutoff at $\Delta E_0 \sim 2V_{\text{eff}}$, which ensures that the statistical expectation value $\langle \Delta E_0 \rangle = \int_0^\infty x P(x) dx$ does not diverge.

Since tunneling rates and their parametric variations are typically studied on a logarithmic scale (i.e., $\log(\Delta E_0)$ rather than $\Delta E_0$ is plotted vs. $1/\hbar$), the relevant quantity to be calculated from Eq. (1.44) and compared to quantum data is not the mean value $\langle \Delta E_0 \rangle$, but rather the average of the logarithm of $\Delta E_0$. We therefore define our "average" level splitting $\langle \Delta E_0 \rangle_g$ as the *geometric* mean of $\Delta E_0$, i.e.

$$\langle \Delta E_0 \rangle_g \equiv \exp\left[\langle \ln(\Delta E_0) \rangle\right] \tag{1.46}$$

and obtain as result the scale defined in Eq. (1.45),

$$\langle \Delta E_0 \rangle_g = \overline{\Delta E_0} \,. \tag{1.47}$$

This expression further simplifies for our specific case of periodically driven systems, where the time evolution operator $U$ is modeled by the dynamics under the effective Hamiltonian

(1.39) over one period $\tau$. In this case, the chaotic eigenphases $\varphi_j^{\pm} \equiv \mathcal{E}_j^{\pm}\tau/\hbar$ are uniformly distributed in the interval $0 < \varphi_j^{\pm} < 2\pi$. We therefore obtain

$$\Delta_c = \frac{2\pi\hbar}{N\tau} \tag{1.48}$$

for the mean level spacing near $E_0$. This yields

$$\langle \Delta\varphi_0 \rangle_g \equiv \frac{\tau}{\hbar}\langle \Delta E_0 \rangle_g = \left(\frac{\tau V_{\text{eff}}}{\hbar}\right)^2 \tag{1.49}$$

for the geometric mean of the ground state's eigenphase splitting. Note that this final result does not depend on how many of the chaotic states do actually participate in the sub-block ($H_{ij}^{\pm}$); as long as this number is sufficiently large to justify the validity of the Cauchy distribution (1.44) (see Ref. [14]), the geometric mean of the eigenphase splitting is essentially given by the square of the coupling $V_{\text{eff}}$ from the ground state to the chaos.

The distribution (1.44) also permits the calculation of the logarithmic variance of the eigenphase splitting: we obtain

$$\left\langle [\ln(\Delta\varphi_0) - \langle \ln(\Delta\varphi_0)\rangle]^2 \right\rangle = \frac{\pi^2}{4}\,. \tag{1.50}$$

This universal result predicts that the actual splittings may be enhanced or reduced compared to $\langle \Delta\varphi_0 \rangle_g$ by factors of the order of $\exp(\pi/2) \simeq 4.8$, independently of the values of $\hbar$ and external parameters. Indeed, we shall show that short-range fluctuations of the splittings, arising at small variations of $\hbar$, are well characterized by the standard deviation that is associated with Eq. (1.50).

### 1.2.5 The role of partial barriers in the chaotic domain

In the previous section, we assumed a perfectly homogeneous structure of the Hamiltonian outside the outermost invariant torus, which allowed us to make a simpe random-matrix ansatz for the chaotic block. This assumption hardly ever corresponds to reality. As was shown in Refs. [9, 10] for the quartic oscillator, the chaotic part of the phase space is, in general, divided into several subregions which are weakly connected to each other through partial transport barriers for the classical flux (see, e.g., Fig. 8 in Ref. [10]). This substructure of the chaotic phase space (which is generally not visible in a Poincaré surface of section) is particularly pronounced in the immediate vicinity of a regular island, where a dense hierarchical sequence of partial barriers formed by broken invariant tori and island chains is accumulating [40, 41, 42].

In the corresponding quantum system, such partial barriers may play the role of "true" tunneling barriers in the same spirit as invariant classical tori. This will be the case if the phase space area $\Delta W$ that is exchanged across such a partial barrier within one classical iteration is much smaller than Planck's constant $2\pi\hbar$ [43], while in the opposite limit $\Delta W \gg 2\pi\hbar$ the classical partial barrier appears completely transparent in the quantum system [44]. Consequently, the "sticky" hierarchical region around a regular island acts, for not extremely small values of $\hbar$, as a dynamical tunneling area and thereby extends the effective

"quantum" size of the island in phase space. This particularly leads to the formation of localized "hierarchical states" [45] which are supported by this sticky phase space region in the surrounding of the regular island.

An immediate consequence of the presence of such partial barriers for resonance-assisted tunneling is the fact that the crticical action variable $I_c$ defining the number $\kappa$ of resonance-assisted steps within the island according to Eq. (1.40) should not be determined from the outermost invariant torus of the island, but rather from the outermost partial barrier that acts like an invariant torus in the quantum system. We find that this outermost quantum barrier is, for not extremely small values of $\hbar$, generally formed by the stable and unstable manifolds that emerge from the hyperbolic periodic points associated with a low-order nonlinear $r$:$s$ resonance. These manifolds are constructed until their first intersection points in between two adjacent periodic points, and iterated $r-1$ times (assuming that no period-doubling of the island chain due to discrete symmetries takes place), such as to form a closed artificial boundary around the island in phase space [46]. As shown in Fig. 1.3, one further iteration maps then this boundary onto itself, except for a small piece that develops a loop-like deformation. The phase space area that is enclosed between the original and the iterated boundary precisely defines the classical flux $\Delta W$ that is exchanged across this boundary within one iteration of the map [40, 41].

The example in Fig. 1.3 shows a boundary that arises from the inner stable and unstable manifolds (i.e. the ones that would, in a near-integrable system, form the inner separatrix structure) emerging from the unstable periodic points of a 4:1 resonance (which otherwise is not visibly manifested in the Poincaré section) in the kicked rotor system. Judging from the size of the flux area $\Delta W$, this boundary should represent the relevant quantum chaos border for the tunneling processes that are discussed in the following section. We clearly see that it encloses a non-negligible part of the chaotic classical phase space, which includes a prominent 10:3 resonance that, consequently, needs to be taken into account for the coupling process between the regular island and the chaotic sea. We thereby naturally arrive at *multi-step* coupling processes across a sequence of several resonances, which would have to be computed for a reliable prediction of the quantum tunneling rates in the semiclassical regime.

### 1.2.6 Multi-resonance processes

...

## 1.3 Application to the kicked rotor

### 1.3.1 Tunneling in the kicked rotor

To demonstrate the validity of our approach, we apply it to the "kicked rotor" model, which is described by the Hamiltonian

$$H(p,q,t) = p^2/2 - K \sum_{n=-\infty}^{\infty} \delta(t-n)\cos q\,. \tag{1.51}$$

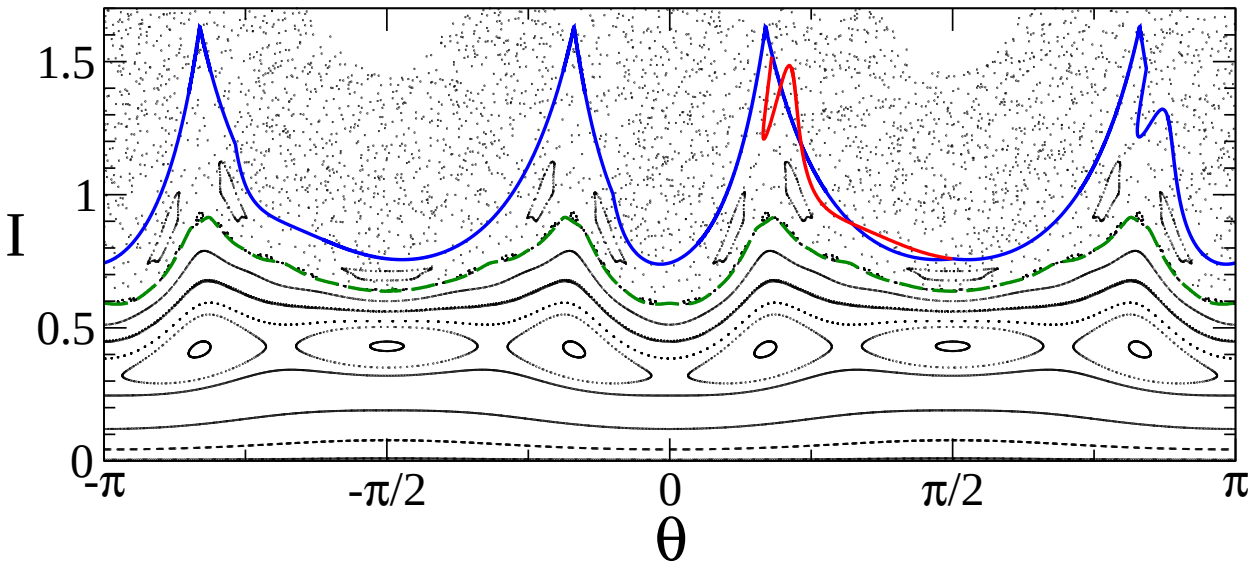


Figure 1.3: Classical phase space of the kicked rotor at $K = 3.4$ in approximate action-angle variables $(I, \theta)$. The solid blue line shows the location of the effective quantum boundary of the central island for the values of Planck's constant that are considered in Section 1.3. This effective boundary is constructed from the stable and unstable manifolds that emerge from the hyperbolic periodic points of the 4:1 resonance. An iteration of this boundary under the classical kicked rotor maps it onto itself, except for the piece between $\theta \simeq 0.15\pi$ and $\theta = 0.5\pi$ which is replaced by the red curve. The phase space area that is enclosed between the original (blue) and the iterated (red) boundary defines the classical flux that is exchanged across this boundary within one iteration of the map. The dashed green line shows, in comparison, the actual classical chaos border defined by the outermost invariant torus of the island.

The classical dynamics of this system is described by the "standard map" $(p, q) \mapsto (p', q')$ with

$$p' = p - K \sin q \tag{1.52}$$
$$q' = q + p' , \tag{1.53}$$

which generates the stroboscopic Poincaré section at times immediately before the kick. The phase space of the kicked rotor is $2\pi$ periodic in position $q$ and momentum $p$, and exhibits, for not too large perturbation strengths $K < 4$, a region of bounded regular motion centered around $(p, q) = (0, 0)$.

The quantum dynamics of the kicked rotor is described by the associated time evolution operator

$$U = \exp\left(-\frac{i}{\hbar}\frac{p^2}{2}\right) \exp\left(-\frac{i}{\hbar} K \cos\hat{q}\right) \tag{1.54}$$

which contains two unitary operators that describe the effect of the kick and the propagation in between two kicks, respectively ($\hat{p}$ and $\hat{q}$ denote the position and momentum operators). Due to the periodicity in $q$, we can apply Bloch's theorem and restrict the consideration to the subspace of states $\psi(q)$ that are $2\pi$-periodic in position, i.e. with $\psi(q + 2\pi) = \psi(q)$.

In order to simplify the quantum eigenvalue problem, we furthermore restrict the choice of Planck's constant to discrete values according to $\hbar = 2\pi/N$ with even integer $N > 0$. For this particular choice, which corresponds to a "quantum resonance" of the kicked rotor [47, 48], the time evolution operator $U$ exhibits, within the above subspace, $2\pi$-periodicity not only in position, but also in momentum. More precisely, the two phase-space translation operators $T_1 = \exp(2\pi i\hat{p}/\hbar)$ and $T_2 = \exp(-2\pi i\hat{q}/\hbar)$ mutually commute with $U$ and with each other when being restricted to the subspace of periodic functions. This allows us to make a Bloch ansatz in momentum as well, i.e., to choose eigenstates $\psi(q) = \psi(q + 2\pi)$ with the additional property

$$\hat{\psi}(p + 2\pi) = \hat{\psi}(p)\exp(i\xi) \tag{1.55}$$

where $\hat{\psi}$ denotes the Fourier transform of $\psi$. Since the subspace of wave functions satisfying periodic boundary conditions in position and the periodicity condition (1.55) in momentum has finite dimension $N$, finite matrices need to be diagonalized in order to obtain the eigenstates of $U$.

Quantum tunneling can take place between the main regular island centred around $(p, q) = (0, 0)$ and its counterparts that are shifted by integer multiples of $2\pi$ along the momentum axis. The spectral manifestation of this classically forbidden coupling process is a finite bandwidth of the eigenphases $\varphi_n \equiv \varphi_n^{(\xi)}$ of $U$ that are associated with the $n$th excited quantized torus within the island. This bandwidth can be characterized by the difference

$$\Delta\varphi_n = |\varphi_n^{(0)} - \varphi_n^{(\pi)}| \tag{1.56}$$

between the eigenphases of the periodic ($\xi = 0$) and the anti-periodic ($\xi = \pi$) state in momentum, which we shall focus on in the following. In this way, we effectively map the tunneling problem to a symmetric double well configuration, with the two wells centred, e.g., around $(p, q) = (0, 0)$ and $(2\pi, 0)$.

### 1.3.2 Eigenphase splittings

Figures 1.4 and 1.5 show the eigenphase splittings $\Delta\varphi_0$ [see Eq. (1.56)] of the kicked rotor for the local "ground state" ($n = 0$) in the central island, i.e. for the state that is most strongly localized around the center of the island, at $K = 2.6, 2.8, \ldots 3.6$. As in Refs. [33, 35], the splittings were calculated with a diagonalization routine for complex matrices that is based on the GMP multiple precision library [49], in order to obtain accurate eigenvalue differences below the ordinary machine precision limit. While on average these splittings decrease exponentially with the number $N = 2\pi/\hbar$ of Planck cells that fit into one Bloch cell, significant fluctuations arise on top of that exponential decrease, which are traced back to the presence of nonlinear resonances.

This is confirmed by the semiclassical prediction of the eigenphase splittings, which is based on the most relevant resonances that are encountered in phase space. In practice, we took those $r$:$s$ resonances into account that exhibit the smallest possible values of $r$ and $s$ for the winding numbers $s/r$ under consideration. In all of the considered cases, the "quantum boundary" of the regular island was defined by the partial barrier that results from the intersections of the inner stable and unstable manifolds associated with the hyperbolic periodic points of the 4:1 resonance (see also Fig. 1.3). While this partial barrier lies rather close to the classical chaos border of the island for $K = 2.6$ (Fig. 1.4), it encloses an appreciable part of the chaotic phase for $K = 3.6$ (Fig. 1.5) including some relevant nonlinear resonances.

We generally find that the quantum splittings are quite well reproduced by our simple semiclassical theory based on nonlinear resonances. In particular, the location and height of prominent plateau structures and peaks in the tunneling rates can, in almost all cases, be quantitatively reproduced through resonance-assisted tunneling. The additional fluctuations of the splittings on a small scale of $N$, however, cannot be accounted for by our approach as they arise from the details of the eigenspectrum in the chaotic block of the Hamiltonian Their average size, however, seems in good agreement with the universal prediction (1.50) for the variance of eigenphase splittings in chaos-assisted tunneling.

### 1.3.3 Direct and resonance-assisted tunneling

Apart from those small-scale fluctuations due to chaos-assisted tunneling, there are also more systematic deviations between the quantum and the semiclassical tunneling rates, which may partially lead to an over- or underestimation of the quantum eigenphase splittings by several orders of magnitude. These deviations are attributed to the approximate nature of the semiclassical approach based on nonlinear resonances, in particular to the simplified structure of the Floquet Hamiltonian shown in Fig. 1.2. This structure is expected to become invalid expecially near the effective chaos border (possibly extended into the chaotic sea due to partial barriers), where the presence of a number of perturbations and additional resonances may give rise to various pathways and couplings to the chaotic sea. Consequently, the last perturbative steps to the chaotic domain [i.e., the last terms in the product in Eq. (1.40)] may not be accurately described by resonance-assisted tunneling. This also concerns single-step tunneling processes in the deep quantum limit of rather large $2\pi\hbar$, being slightly smaller than the area enclosed by the island, where substructures due to nonlinear resonances are generally not expected to play an important role.

Bäcker et al. [20] recently proposed a simple but accurate method to predict tunneling rates in this "quantum" regime of rather large $\hbar$. This method relies on the explicit construction of a good integrable approximation $H_0(p,q)$ to the time-dependent dynamics (see Sec. 1.2.1), which then allows one, by quantum or semiclassical diagonalization, to determine the unperturbed eigenstates $|n\rangle$ within the regular island, and to construct the projectors $P_{\rm reg}$ and $P_{\rm ch}$ onto the subspaces of the Hilbert space that are associated with the regular and chaotic parts, respectively, of the classical phase space. The "direct" regular-to-chaotic tunneling rate $\Delta\varphi_n^{(d)}$ of the $n$th quantized state within the island is then evaluated by a simple application of the quantum time evolution operator $U$ over one period of the driving according to

$$\Delta\varphi_n^{(d)} = ||P_{\rm ch}(U-U_0)|n\rangle||^2 \tag{1.57}$$

with $U_0 \equiv \exp(-i\tau H_0/\hbar)$. Very good agreement between this prediction and numerically computed quantum tunneling rates was found for quantum maps that were designed such as to yield a "clean" mixed regular-chaotic phase space, containing a regular island and a chaotic region which both do not exhibit appreciable substructures [20], as well as for the mushroom billiard [21]. In more generic situations, where nonlinear resonances are manifested within the regular island, this approach yields reliable predictions only in the regime of large $\hbar$ in which modifications of the integrable approximation $H_0$ due to such resonances are not relevant for the quantum tunneling process. This "direct" regular-to-chaotic tunneling approach can therefore be seen as complementary to resonance-assisted tunneling.

In view of this fact, direct and resonance-assisted tunneling (in its improved form as described in Sec. 1.2.3) were recently combined to yield a powerful tool for the semiclas-

sical determination of tunneling rates in mixed systems [50]. The main idea behind this combination is that nonlinear resonances may induce perturbative couplings between locally quantized states *within* the regular island, whereas the coupling to chaotic states beyond the chaos border is more reliably evaluated with direct tunneling. Technically, this amounts to replacing $\Delta\varphi_n^{(0)}$ in Eq. (1.38) with $\Delta\varphi_n^{(d)}$ from Eq. (1.57). Figure 1.6 shows the resulting prediction for the eigenphase splittings of the quantum kicked rotor at $K = 3.5$ [50] (see Fig. 1.1 for the corresponding classical phase space) in comparison with the exact quantum splittings and with the prediction resulting from "plain" resonance-assisted tunneling. We see that the inclusion of direct tunneling gives rise to a significant quantitative improvement in the prediction of the quantum tunneling rates, which now appears to become possible on the level of individual peaks.

### 1.3.4 The role of bifurcations

...

## 1.4 Conclusion

...

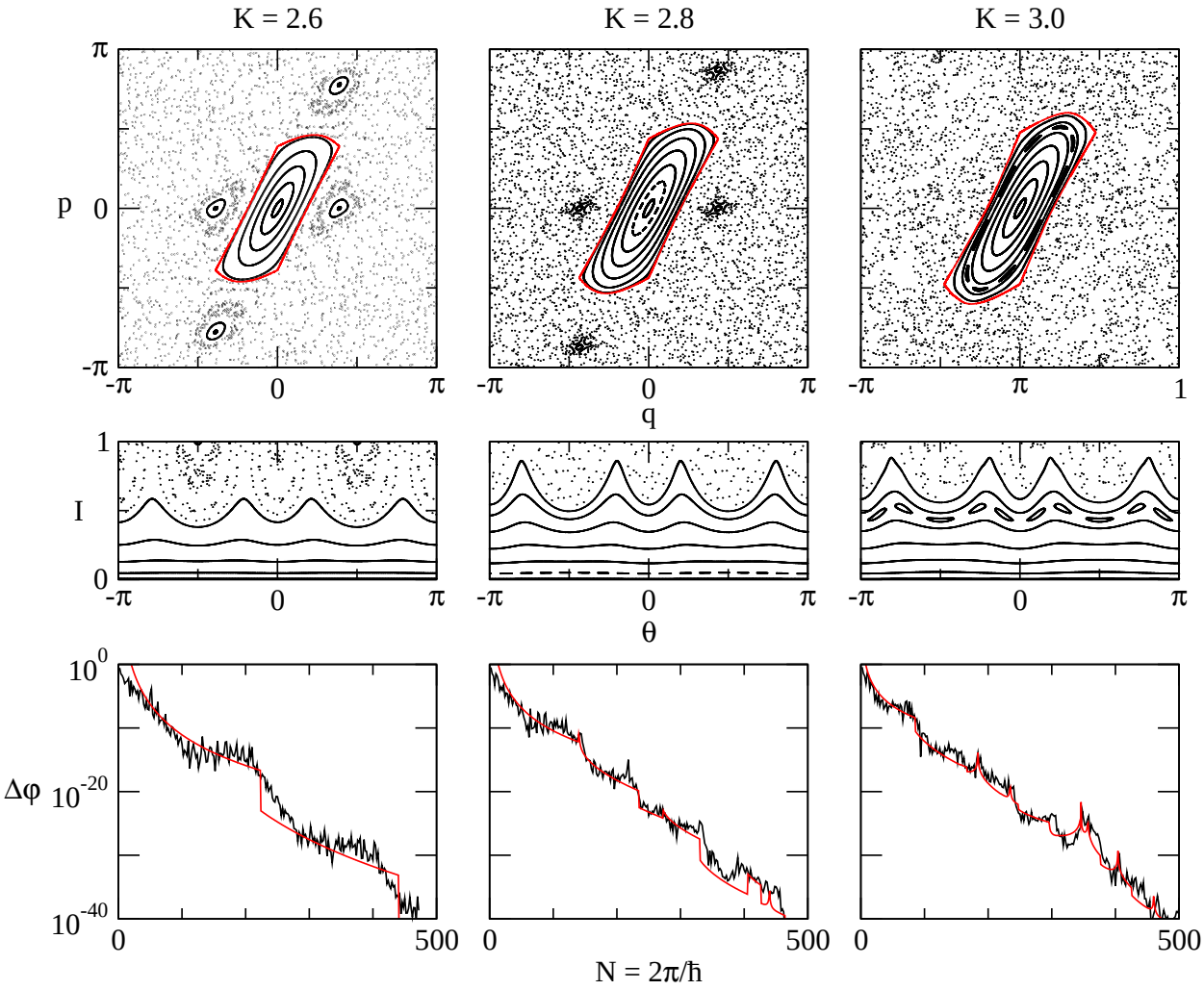


Figure 1.4: Quantum and semiclassical splittings in the kicked rotor model for $K = 2.6$ (left column) $K = 2.8$ (central column), and $K = 3$ (right column). The upper and middle panels show the classical phase space in the original phase space variables $p$ and $q$, with the red curve marking the effective quantum boundary of the island, and in approximate action-angle variables $I$ and $\theta$. The lower panels display the quantum and semiclassical eigenphase splittings (black and red lines, respectively) of the ground state in the central regular island. For the semiclassical splittings, we used the 18:5 resonance for $K = 2.6$, the 10:3 and 14:4 resonances for $K = 2.8$, and the 10:3, 14:4, 16:5, and 22:7 resonances for $K = 3$.

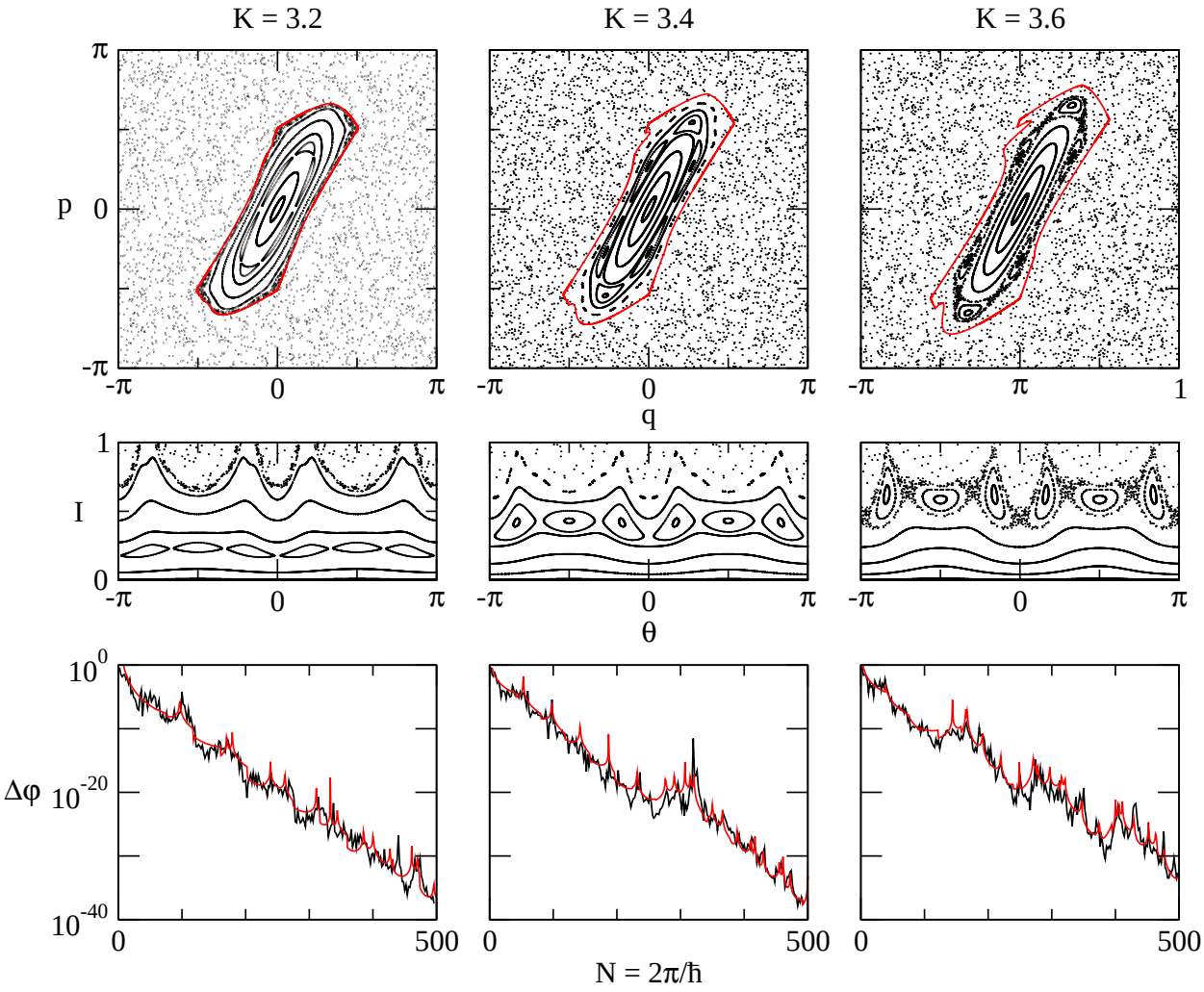


Figure 1.5: Same as Fig. 1.4 for $K = 3.2$, $K = 3.4$, and $K = 3.6$. For the semiclassical splittings, we used the 6:2 and 10:3 resonances for $K = 3.2$, the 6:2, 10:3, and 14:5 resonances for $K = 3.4$, and the 6:2 and 8:3 resonances for $K = 3.6$.

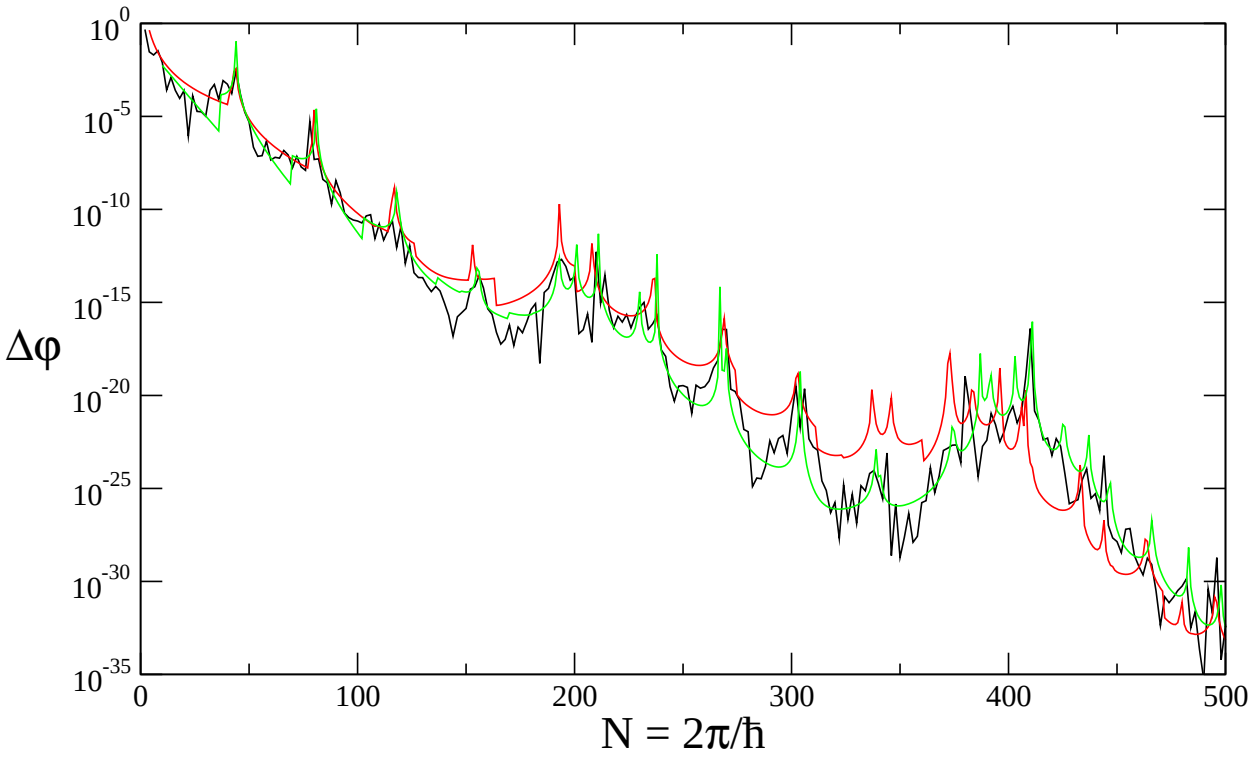


Figure 1.6: Direct and resonance-assisted tunneling in the kicked rotor model for $K = 3.5$ (see Fig. 1.1 for the classical phase space). As ins Figs. 1.4 and 1.5, the black and red lines represent, respectively, the quantum splittings and the semiclassical prediction based on our approach, where we take into account the 6:2, 8:3, 10:3, and 14:5 resonances. The green line shows the prediction that is obtained from a combination of direct regular-to-chaotic tunneling and resonance-assisted tunneling, which is taken from Ref. [50]. We see that the accuracy of the reproduction of the quantum eigenphase splittings is significantly improved in the combined approach where the final coupling to the chaotic sea is evaluated by means of the projection method presented in Ref. [20].

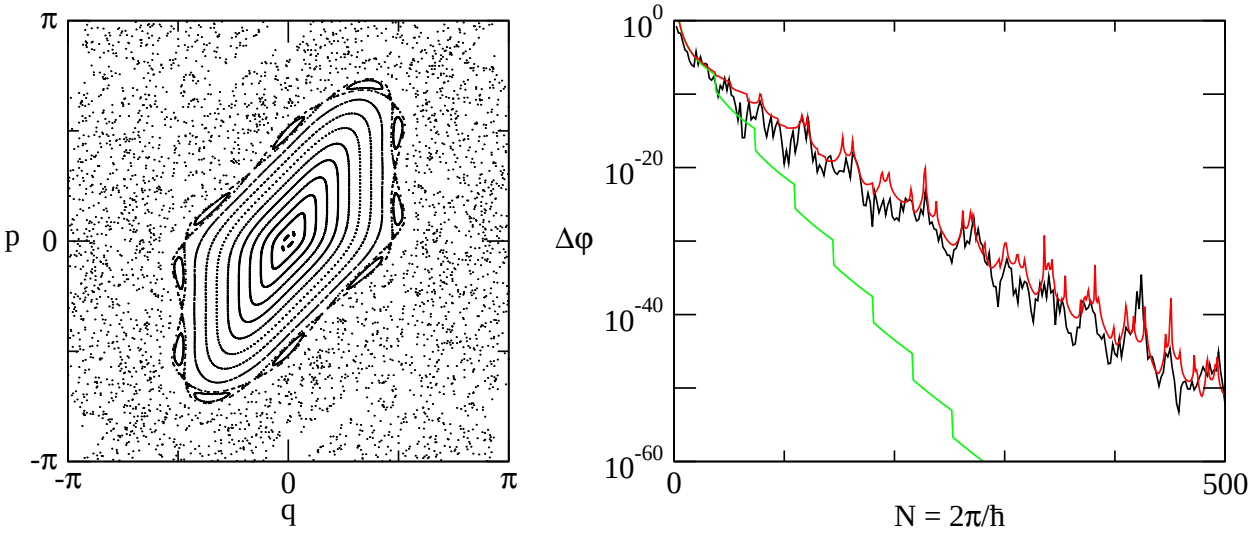


Figure 1.7: Resonance-assisted tunneling in the kicked rotor at a bifurcation. The left panel shows the classical phase space for $K = 2$, which contains a prominent 10:2 resonance close to the border of the island, and the right panel displays the corresponding quantum eigenphase splittings (black line). Semiclassical calculations of the splittings (red and green lines) were carried out using the 10:2 resonance only (green line) as well as a combination of the 4:1 resonance and the 10:2 resonance, the former emerging at the island's center right at $K = 2$. The parameter $\tilde{v}_1$ associated with that 4:1 resonance [see Eq. (1.36)] were determined from the classical phase space at $K = 2.001$.

## References


[1] M. J. Davis and E. J. Heller, J. Chem. Phys. **75**, 246 (1981).
[2] W. K. Hensinger, H. Häffner, A. Browaeys, N. R. Heckenberg, K. Helmerson, C. McKenzie, G. J. Milburn, W. D. Phillips, S. L. Rolston, H. Rubinsztein-Dunlop, and B. Upcroft, Nature **412**, 52 (2001).
[3] D. A. Steck, W. H. Oskay, and M. G. Raizen, Science **293**, 274 (2001).
[4] S. Creagh, in *Tunneling in Complex Systems*, edited by S. Tomsovic (World Scientific, Singapore, 1998), pp. 1–65.
[5] L. D. Landau and E. M. Lifshitz, *Quantum Mechanics: Non-Relativistic Theory* (Pergamon, Oxford, 1958).
[6] S. C. Creagh, J. Phys. A **27**, 4969 (1994).
[7] W. A. Lin and L. E. Ballentine, Phys. Rev. Lett. **65**, 2927 (1990).
[8] O. Bohigas, D. Boosé, R. Egydio de Carvalho, and V. Marvulle, Nucl. Phys. A **560**, 197 (1993).
[9] O. Bohigas, S. Tomsovic, and D. Ullmo, Phys. Rep. **223**, 43 (1993).
[10] S. Tomsovic and D. Ullmo, Phys. Rev. E **50**, 145 (1994).
[11] E. Doron and S. D. Frischat, Phys. Rev. Lett. **75**, 3661 (1995).
[12] S. D. Frischat and E. Doron, Phys. Rev. E **57**, 1421 (1998).
[13] F. Grossmann, T. Dittrich, P. Jung, and P. Hänggi, Phys. Rev. Lett. **67**, 516 (1991).
[14] F. Leyvraz and D. Ullmo, J. Phys. A **29**, 2529 (1996).
[15] A. Mouchet, C. Miniatura, R. Kaiser, B. Grémaud, and D. Delande, Phys. Rev. E **64**, 016221 (2001).
[16] A. Mouchet and D. Delande, Phys. Rev. E **67**, 046216 (2003).
[17] V. A. Podolskiy and E. E. Narimanov, Phys. Rev. Lett. **91**, 263601 (2003).
[18] V. A. Podolskiy and E. E. Narimanov, Opt. Lett. **30**, 474 (2005).
[19] A. Bäcker and R. Ketzmerick, private communication.
[20] A. Bäcker, R. Ketzmerick, S. Löck, and L. Schilling, Phys. Rev. Lett. **100**, 104101 (2008).
[21] A. Bäcker, R. Ketzmerick, S. Löck, M. Robnik, G. Vidmar, R. Höhmann, U. Kuhl, and H.-J. Stöckmann, Phys. Rev. Lett. **100**, 174103 (2008).
[22] A. M. Ozorio de Almeida, J. Phys. Chem. **88**, 6139 (1984).
[23] T. Uzer, D. W. Noid, and R. A. Marcus, J. Chem. Phys. **79**, 4412 (1983).
[24] L. Bonci, A. Farusi, P. Grigolini, and R. Roncaglia, Phys. Rev. E **58**, 5689 (1998).
[25] O. Brodier, P. Schlagheck, and D. Ullmo, Phys. Rev. Lett. **87**, 064101 (2001).
[26] O. Brodier, P. Schlagheck, and D. Ullmo, Ann. Phys. **300**, 88 (2002).
[27] S. Keshavamurthy, J. Chem. Phys **122**, 114109 (2005).
[28] S. Keshavamurthy, Phys. Rev. E **72**, 045203(R) (2005).
[29] A. J. Lichtenberg and M. A. Lieberman, *Regular and Stochastic Motion* (Springer-Verlag, New York, 1983).
[30] In order no to overload the notation, we use the same symbol $H$ for the Hamiltonian in the original phase-space variables $(p, q)$ and in the action-angle variables $(I, \theta)$.
[31] This step involves, strictly speaking, another time-dependent canonical transformation $(I, \vartheta) \mapsto (\widetilde{I}, \widetilde{\vartheta})$ which slightly modifies $I$ and $\vartheta$ (see also Ref. [26]).
[32] Exceptions from this general rule typically arise in the presence of discrete symmetries that, e.g., forbid the formation of resonance chains with an odd number of sub-islands and therefore lead to $V_1 = 0$ for an $r$:$s$ resonance with an odd $r$.
[33] C. Eltschka and P. Schlagheck, Phys. Rev. Lett. **94**, 014101 (2005).
[34] S. Tomsovic, M. Grinberg, and D. Ullmo, Phys. Rev. Lett. **75**, 4346 (1995).
[35] P. Schlagheck, C. Eltschka, and D. Ullmo, in *Progress in Ultrafast Intense Laser Science I*, edited by K. Yamanouchi, S. L. Chin, P. Agostini, and G. Ferrante (Springer, Berlin,

2006), pp. 107–131.
[36] A. Mouchet, C. Eltschka, and P. Schlagheck, Phys. Rev. E **74**, 026211 (2006).
[37] G. D. Birkhoff, *Dynamical Systems* (Am. Math. Soc., New York, 1966).
[38] F. G. Gustavson, Astron. J. **71**, 670 (1966).
[39] This involves, strictly speaking, another cannonical transformation of $P$ and $Q$ to the frame that co-rotates with the resonance.
[40] R. S. MacKay, J. D. Meiss, and I. C. Percival, Phys. Rev. Lett. **52**, 697 (1984).
[41] R. S. MacKay, J. D. Meiss, and I. C. Percival, Physica **13D**, 55 (1984).
[42] J. D. Meiss and E. Ott, Phys. Rev. Lett. **55**, 2742 (1985).
[43] N. T. Maitra and E. J. Heller, Phys. Rev. E **61**, 3620 (2000).
[44] More precisely, the authors of Ref. [43] claim that $\Delta W$ has to be compared with $\pi\hbar$ in order to find out whether or not a given partial barrier is transparent in the quantum system.
[45] R. Ketzmerick, L. Hufnagel, F. Steinbach, and M. Weiss, Phys. Rev. Lett. **85**, 1214 (2000).
[46] This construction is also made in order to obtain the phase space areas $S^{\pm}_{r:s}$ that are enclosed by the outer and inner separatrix structures of an $r$:$s$ resonance, and that are needed in order to compute the mean action variable $I_{r:s}$ and the coupling strength $V_{r:s}$ of the resonance according to Eqs. (1.26) and (1.27).
[47] F. Izrailev and D. Shepelyansky, Sov. Phys. Dokl. **24**, 996 (1979)).
[48] S. Fishman, I. Guarneri, and L. Rebuzzini, Phys. Rev. Lett. **89**, 084101 (2002).
[49] `http://gmplib.org`.
[50] S. Löck, A. Bäcker, R. Ketzmerick, and P. Schlagheck, arXiv:0906.4893 (2009).